Contract No.:

This manuscript has been authored by Savannah River Nuclear Solutions (SRNS), LLC under Contract No. DE-AC09-08SR22470 with the U.S. Department of Energy (DOE) Office of Environmental Management (EM).

High Vacuum Measurement and Calibration Concerns, Molecular Flow Fluid Transients

Robert A. Leishear, PhD, P. E.
robert.leishear@srnl.doe.gov
Savannah River Nuclear Solutions
Savannah River Site
Aiken, SC, 29808

Nickolas A. Gavalas
nickolas.gavalas@srnl.doe.gov
Savannah River National Laboratory
Savannah River Site
Aiken, SC, 29808

ABSTRACT

High vacuum pressure measurements and calibrations approaching 1×10^{-8} Torr are problematic. Specifically, accuracies change for different vacuum gauge designs when pressures are suddenly lowered in a vacuum system. How can gauges perform like this? To answer this question, a brief system description is first required. Calibrations were performed using a vacuum calibration chamber with attached vacuum gauges. To control chamber pressures, vacuum pumps decreased the chamber pressure while nitrogen bottles increased the chamber pressure. By balancing these opposing pressures, equilibrium in the chamber was maintained at selected set point pressures to perform calibrations. When pressures were suddenly decreased during set point adjustments, a sudden rush of gas from the chamber also caused a surge of gas from the gauges to decrease the pressures in those gauges. Gauge pressures did not return to equilibrium as fast as chamber pressures due to the sparse distribution of gas molecules in the system. This disparity in the rate of pressure changes caused the pressures in different gauges to be different than expected. This discovery of a new theory was experimentally proven to demonstrate that different gauge designs return to equilibrium at different rates, and gauge accuracies are consequently affected differently due to fluid transients in molecular flow.

KEYWORDS

Fluid transients, molecular flow, ion gauge, spinning rotor gauge, capacitance diaphragm gauge, cold cathode gauge, vacuum measurement, vacuum calibration.

1. INTRODUCTION

Research was performed in high vacuum systems at Savannah River Standards Laboratory (SRSL) in South Carolina using several different types of vacuum gauges, which included spinning rotor gauges (SRGs), capacitance diaphragm gauges (CDGs), ion gauges (IGs) and cold cathode gauges (CCGs). Although performance of each gauge design varied, a symptomatic problem was observed when calibrations were performed. The accuracies of all gauges were

affected when pressures in the system were suddenly decreased to low vacuum pressures. Accuracies of different gauges were compared through testing and by evaluating the uncertainties for different gauges, where multiple gauges were installed while measuring vacuums. To understand this phenomenon, discussions of uncertainty and high vacuums along with system and gauge descriptions are required to introduce test results and the analysis of data. Numerous tests were performed for this investigation to understand process anomalies and ensure reproducibility of results. Only a representative selection of data is presented herein.

Material and test equipment numbers (M&TE numbers) for gauges are provided herein for identification and traceability to original research data, but have little direct application to this presentation.

SRSL operates in accordance with *ANSI/ISO 17025* [1] and is accredited by the National Voluntary Laboratory Accreditation Program (NVLAP) for vacuum calibration services, as well as other calibration services.

2. UNCERTAINTY ANALYSIS

Uncertainty analysis was integral to this study, and was performed in accordance with established uncertainty techniques available in *JCGM 100* [2]. Details of uncertainty analysis that were performed for this study are largely excluded from this discussion, but uncertainties are mentioned as applicable to gauge performance. A k value of two is used for SRSL calibrations. For $k = 2$, the confidence level equals 95.45 %. A value of $k = 2$ is recommended by the National Institute of Standards and Technology, NIST [3] and the American Society of Mechanical Engineers, ASME [4].

2.1 Standard Deviation

The standard deviation, σ, determines the variation of a series of N values, or measurements, from their mean value, μ [5]. For vacuum measurements, these statistical values are the actual, or true, calculated *ACT* values. To obtain true values, measured readings, *RDG,* are first read directly from vacuum gauge controller displays. These measured values are then mathematically manipulated using Excel® spread sheets to obtain the actual values, as shown in Table 1.

The equations used to calculate *ACT* values were supplied by the Primary Standards Laboratory, PSL, in Sandia, New Mexico. PSL calibrated ion gauges and CDGs for SRSL. For example, the actual values for some of the measurements calculated from a CDG (M&TE number: SL-457K) were determined from the equation,

$$ACT = 9.62 \cdot RDG^1 - 5.09 \cdot RDG^2 + 1.99 \cdot RDG^3 \quad . \tag{1}$$

As another example, the actual values for an ion gauge (M&TE number: SL-457U) were determined as

$$ACT = 3.53 \cdot RDG + 1.86(\log RDG) + 0.49 \cdot (\log RDG)^2 + 0.06 \cdot (\log RDG)^3$$
$$+0.002 \cdot (\log RDG)^4 \quad . \tag{2}$$

Once the true values were determined, the mean and the standard deviation were expressed as

$$\mu = \frac{\sum_{i=1}^{N} ACT_i}{N}, \text{ and} \tag{3}$$

$$\sigma = \sqrt{\frac{\sum_{i=1}^{N} \mu - ACT_i}{N-1}}. \tag{4}$$

Equation 4 describes the standard deviation and is based on the symmetrical normal distribution, which is frequently referred to as a bell shaped curve.

Nominal	SL-457U	SL-457U	SL-457T	SL-457T	Difference	Tolerance
Target	Display Torr	Actual Torr	Display Torr	Actual Torr	% of Reading	Torr
1.41e-8	2.4900E-08	2.4344E-08	1.270E-08	1.2227E-08	-91.7%	6.8961E-10
2.38e-8	3.3900E-08	3.3108E-08	2.050E-08	1.9736E-08	-61.5%	1.1132E-09
4.63e-8	5.9500E-08	5.8111E-08	4.650E-08	4.4755E-08	-25.0%	2.5250E-09
1.61e-7	1.6600E-07	1.6267E-07	1.510E-07	1.4537E-07	-7.7%	8.1993E-09
4.86e-7	5.1700E-07	5.0838E-07	4.970E-07	4.7886E-07	-2.3%	2.6987E-08
1.16e-6	1.1500E-06	1.1308E-06	1.130E-06	1.0889E-06	-0.1%	6.1359E-08
4.81e-6	5.3400E-06	5.2147E-06	5.260E-06	5.0632E-06	0.9%	2.8562E-07
1.09e-5	1.0200E-05	9.9149E-06	1.000E-05	9.6246E-06	0.9%	5.4300E-07
4.68e-5	4.4300E-05	4.2767E-05	4.330E-05	4.2001E-05	1.2%	2.3512E-06
9.73e-5	9.2600E-05	8.9681E-05	9.220E-05	9.0727E-05	2.7%	5.0065E-06
4.68e-5	4.4300E-05	4.2767E-05	4.310E-05	4.1804E-05	0.8%	2.3403E-06
1.09e-5	4.3000E-05	4.1512E-05	4.200E-05	4.0724E-05	1.2%	2.2806E-06
1.16e-6	1.6200E-06	1.5917E-06	1.570E-06	1.5128E-06	-1.4%	8.5251E-08
4.86e-7	3.8900E-07	3.8230E-07	3.590E-07	3.4583E-07	-6.5%	1.9494E-08
1.61e-7	1.9000E-07	1.8629E-07	1.670E-07	1.6079E-07	-11.6%	9.0681E-09
4.63e-8	6.3300E-08	6.1830E-08	4.730E-08	4.5524E-08	-30.7%	2.5684E-09
2.38e-8	3.7100E-08	3.6228E-08	2.360E-08	2.2719E-08	-53.5%	1.2815E-09
1.41e-8	IG	3.0200E-08	2.9503E-08	1.560E-08	1.5019E-08	-89.1%

Table 1. Typical calibration data (M&TE numbers: SL-457U and SL-457T).

3.3 Uncertainty

The total expanded uncertainty (U) is used for SRSL calibrations, and includes uncertainties associated with the installed reference calibration standards, u_{ref}, combined with the uncertainties of the gauge being calibrated, u_{UUT}, and the uncertainties of the system response, u_{SYS}, which includes temperature effects, other instrumentation uncertainties, gas properties, flow rate effects, etc. The uncertainty is expressed as

$$U = k \cdot \sqrt{\sum u_{REF}^2 + \sum u_{UUT}^2 + \sum u_{SYS}^2}, \quad (5)$$

where more detail for calculating uncertainties are available in references *JCGM 100* [2], *ISO 3567* [6] and *ISO 27893* [7].

To determine U, the expanded uncertainty (U_{ref}) is used for SRSL calibrations and equals the coverage factor (k) times the square root of the sum of the squares (*RSS*) of the standard uncertainties (u_{REF}) for the identifiable Type A and Type B components of error in the measurement process. Standard uncertainties that are statistically derived (i.e., standard deviations, σ) are identified as Type A uncertainties. Standard uncertainties that are non-statistically derived (i.e., engineering judgment, manufacturer's specs, handling effects, environmental conditions, uncertainties from calibration certificates, and estimates of drift) are identified as Type B uncertainties. Accordingly, both accuracy and precision are tacitly included in the expanded uncertainty used herein. For this research, an important fact is that if the accuracy improves, the uncertainty improves. The expanded uncertainty is expressed as

$$U_{ref} = k \cdot \sqrt{\sum u_{REF}^2}. \quad (6)$$

Similarly, for gauges to be calibrated and for comparisons to SRSL standards,

$$U_{UUT} = k \cdot \sqrt{\sum u_{UUT}^2}. \quad (7)$$

4. VACUUM CONCEPTS

If required, aspects of vacuum systems pertinent to this study can be described through a definition of terms and systems as described by Varian® [8].

4.1 Conversion Factors

Torr are the common units used by national laboratories, such as PSL and SRSL, and their customers. Appropriate conversion factors for vacuum are:

1 atmosphere = 760 Torr
100 Pascals = 100 Newtons /meter^2 = 1 millibar = 0.75 Torr
1 Torr = 1 mm of Hg (mercury)
1 millitorr = 1 micron of Hg

4.2 High Vacuum

Higher vacuums have lower absolute pressures, i.e., the lower the pressure, the higher the vacuum. The system used for this research has a high vacuum limit, or lowest operating pressure,

of approximately 1×10^{-8} Torr, as measured by ion gauges. Pressures occasionally lower to approximately 9×10^{-9} Torr, but these lower pressures are attributed to a pumping action of ions known to occur in ion gauges when these gauges operate continuously without system pressure changes.

4.3 Mean Free Path

The mean free path depends on the molecular density, where these two variables are related in Table 2 [9]. Note that at 7.6×10^{-6} Torr, molecules travel for 6.5 m before hitting another molecule. Accordingly, pressure in molecular flow is not a primary driver for flow.

Pressure	Molecules per cm^3	Mean Free Path, m
760 Torr (1 atmosphere)	2.5×10^{19}	6.5×10^{-8}
7.6×10^{-1} Torr	2.5×10^{16}	6.5×10^{-5}
7.6×10^{-3} Torr	2.5×10^{14}	6.5×10^{-3}
7.6×10^{-6} Torr	2.5×10^{11}	6.5
7.6×10^{-11} Torr	2.5×10^{6}	6.50×10^{5}

Table 2. Mean free path, molecular density and vacuum pressures.

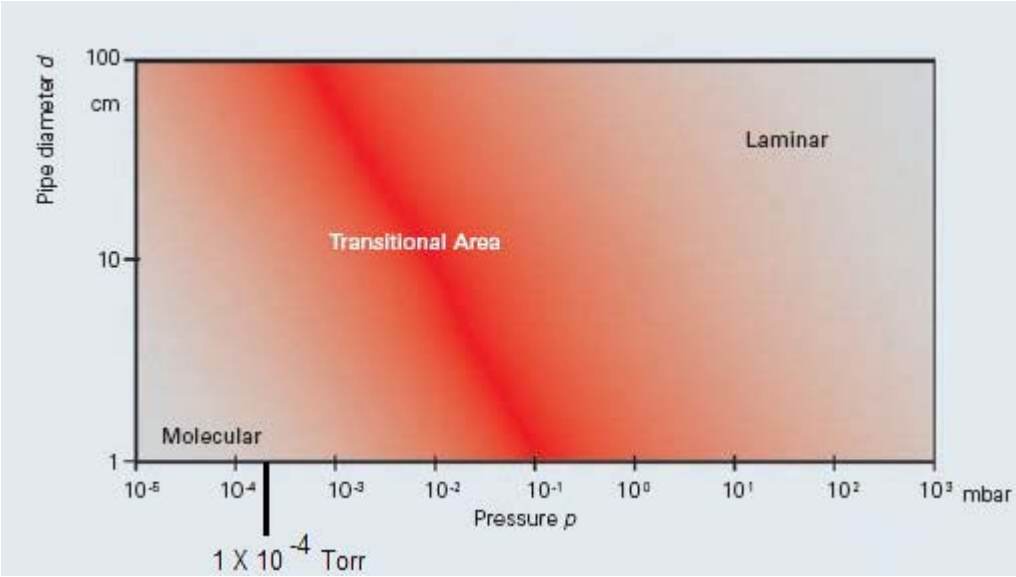

Figure 1. Types of flow in vacuum systems [10] (Reprinted by permission of Oerlikon Leybold Vacuum).

4.4 Conductance

Conductance describes flow in vacuum systems and quantifies the ability of tubing to allow a given volume of gas to pass through in a given time. Pfeiffer Vacuum provides a graph (Fig. 1) to describe different types of flow in vacuum systems, i.e., laminar, transitional and molecular. For the research performed here, test pressures were all below 1×10^{-4} Torr, which means that all

flows in tubing were molecular. At high vacuums, molecular flow occurs due to the random motion of molecules, where long mean free paths result in molecules striking the tubing walls more often than striking other molecules. Leybold Vacuum [11] provides an equation to find conductance, C, in tubing, such that

$$C = \frac{135 \cdot d^4 \cdot \left(\frac{p_1+p_2}{2}\right)}{L} + \frac{12.1 \cdot d^3}{L} \cdot \frac{1+192 \cdot d \cdot \left(\frac{p_1+p_2}{2}\right)}{1+237 \cdot d \cdot \left(\frac{p_1+p_2}{2}\right)} l/s, \tag{8}$$

where d is the inside tubing diameter (cm), L is the pipe length (cm), $L \geq 10 \times d$, p_1 is the upstream pressure (mbar), and p_2 is the downstream pressure (mbar).

Figure 2. Vacuum system and controllers.

5. SYSTEM DESCRIPTION

The system used for calibrations and testing was an Automated Vacuum Gauge Calibrator, VGMS-101, which was manufactured by Vacuum Technology, Inc. (VTI). The general layout of the system is shown in Fig. 2. Figure 3 provides a process and instrumentation drawing of the system as a basis for discussion, where most of the connecting tubing between components is ¼

inch (0.64 cm) stainless steel, and connections to the calibration chamber are 1-3/8 inch (3.49 cm) stainless steel tubing.

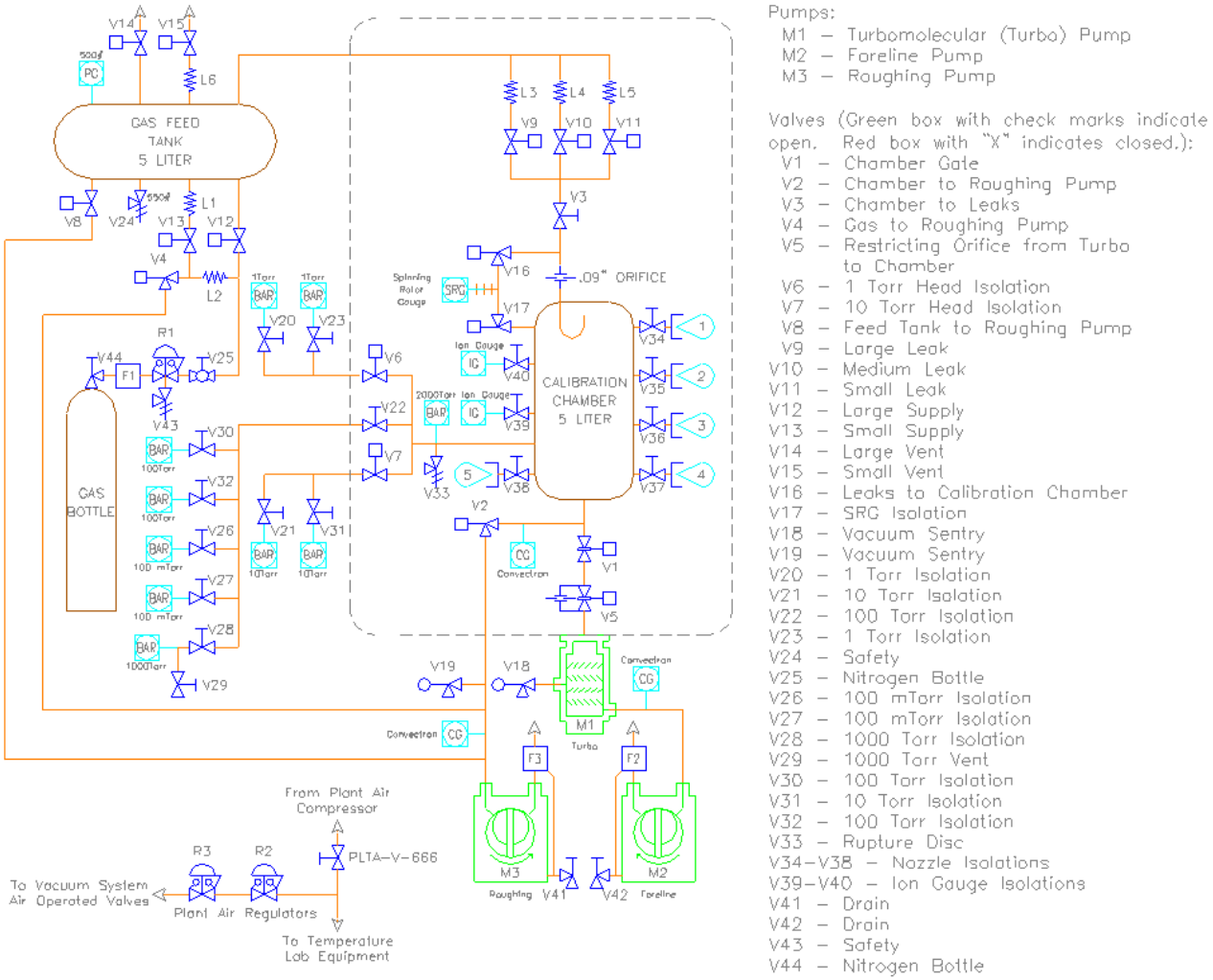

Figure 3. Vacuum system process and instrumentation drawing (Reprinted by permission of Vacuum Technology Incorporated, Oak Ridge, Tennessee).

Calibrations can be performed in automatic mode to obtain pressures at many set points, or calibrations may be performed manually to select each set point. Manual calibrations will be discussed here, where most of the data for this testing was collected using manual calibration techniques. For manual calibrations, valves and pumps are selected and operated one at a time as required, using a computer screen interface that is comparable to Fig. 3.

To initially evacuate the chamber, the roughing pump, M3, is used. Then, to maintain the calibration chamber at high vacuum, valves are opened between the gas feed tank, the calibration

chamber and two operating vacuum pumps, i.e., the foreline pump, M1, and the turbomolecular (turbo) pump, M2.

5.1 Gas Flow Between the Feed Tank and Chamber

Referring to Fig. 3, the gas feed tank provides nitrogen to the chamber during calibrations. To do so, pressure is controlled in the feed tank using valve V8 to provide suction and valve V13 to provide pressurized nitrogen from the gas bottle. Gas travels at sub-sonic velocity to the leaks at valves V10 and V11, which are selected for different flow control. Installed in the tubing, leaks are cylinders with small diameter bores that permit flow to pass at specific flow rates. Since pressure ratios greater than ≈ 0.53 across an orifice result in sonic flows [12], choked flow will occur inside the leaks. Nitrogen will flow through the leaks at 349 m/s at 20° C, which is within the controlled temperatures range of the Vacuum Lab at SRSL. The geometry of the selected leak inherently results in a supersonic flow downstream of that leak, and a standing shock occurs downstream of the leak. Downstream of the shock, flow returns to a subsonic velocity before entering the chamber.

5.2 Gas Flow From the Chamber Through the Pumps

Referring again to Fig. 3, valves V1 and V5 are opened to the turbo and foreline pumps during calibrations to withdraw nitrogen from the chamber. The turbo pump operates similar to a jet turbine and is capable of producing higher vacuum than the foreline pump. The continuous duty foreline pump and start-up roughing pumps are of identical design, where they both contain oil reservoirs to trap contaminants.

5.3 Types of Gauges

Several types of gauge designs were considered with respect to fluid transients, and are discussed briefly. For the various gauges that were tested, fluid transient anomalies were only observed at very low pressures approaching 1×10^{-8} Torr. This observation was critical to conclusions with respect to molecular flow, where transient effects only occurred due to sudden pressure drops down to low pressures. Accordingly, various gauges are considered here.

Also of note, several gauges were used as standards to perform calibrations. The uncertainties for each of these standards were traceable to primary standards that are maintained by national laboratories, such as NIST. Primary standards are maintained by national laboratories to ensure that uncertainties are precisely known through comparison. This traceability ensures the accuracy of standards that were used by Savannah River Standards Laboratory during this testing.

6. CAPACITANCE DIAPHRAGM GAUGES

Capacitance diaphragm gauges measure the change in capacitance that occurs when a vacuum deflects an Inconel diaphragm to induce a measurable change in capacitance, as shown in Fig. 4. CDGs used as SRSL standards are MKS instruments, Model 690, Baratrons.

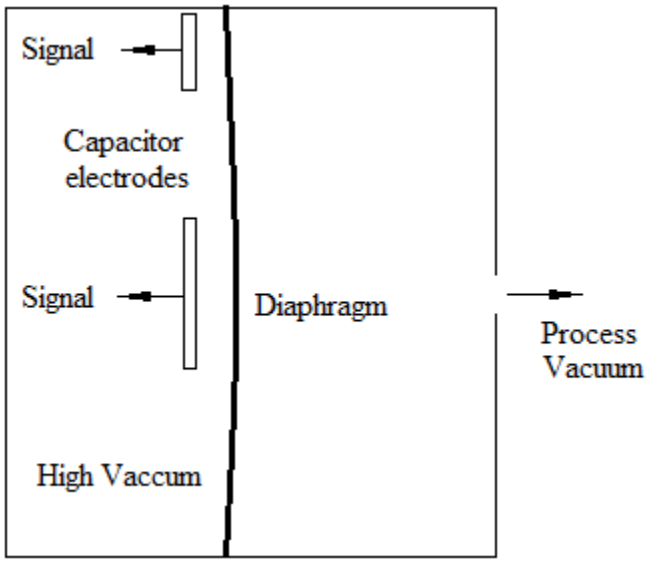

Figure 4. CDG operation [13] (Adapted by permission of Omega Engineering, Inc.).

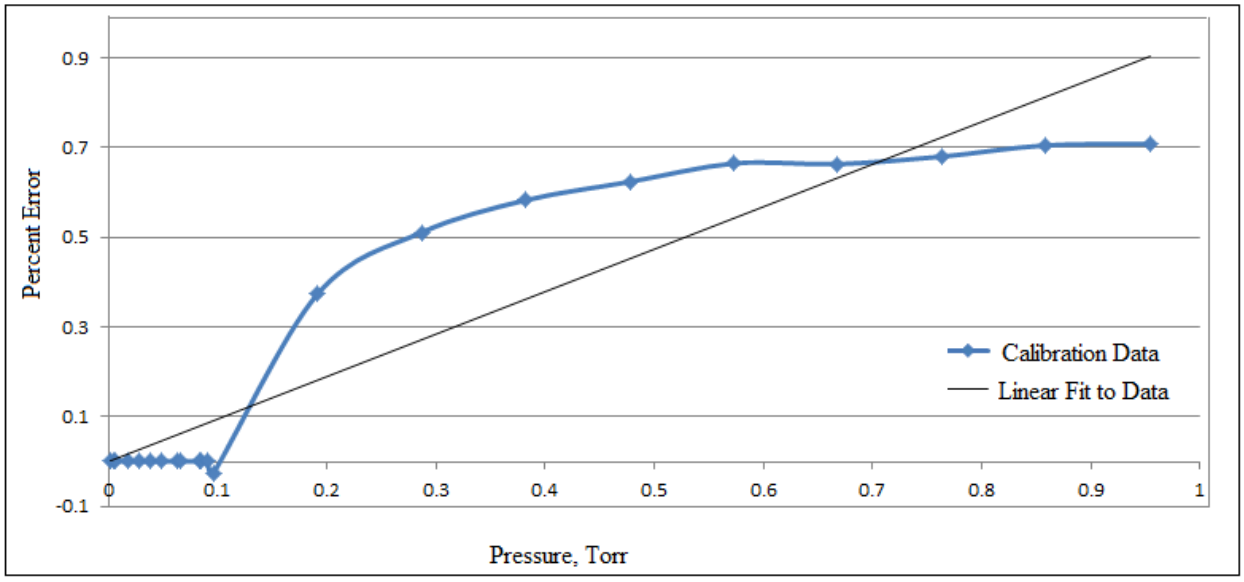

Figure 5. Typical CDG calibration data (1 Torr gauge shown, M&TE number: 20.2053-PE-C).

Hysteresis occurs in some instruments when mechanical components are stressed, where their mechanical properties differ as the stress is relieved. That is, in some pressure instruments,

the measured pressures differ when increasing or decreasing the applied pressures. In general, CDGs are considered to have negligible hysteresis effects.

6.1 CDG Calibrations

Actual values for pressures are determined as discussed in the derivation of Eq. (1). Errors associated with a typical CDG calibration are shown in Fig. 5.

6.2 CDG Test Results

A 100 millitorr Baratron CDG was used for this investigation (M&TE number: SL-457K). The installed CDG was used as a cross check to validate gauge operations, where all of the gauges overlap for a few pressures in a small range (near $1 \times E^{-4}$ Torr). As shown in Table 3, all gauges were within the specified uncertainties. Pressures were raised, lowered, and raised again during this test. Pressures were negligibly affected by sudden pressure drops at these pressures.

SRG, Torr	SRG Uncertainty	IG, Torr	IG Uncertainty	CDG, Torr	CDG Uncertainty	Error, IG to CDG	Error, SRG to CDG
1.106E-04	2.04 %	1.108E-04	0.0039	1.105E-04	12.33 %	0.27 %	0.088 %
4.29E-04	2.04 %	4.767E-04	---	4.319E-04	3.37 %	10.37 %	-0.46 %
1.106E-04	2.04 %	1.108E-04	---	1.042E-04	12.33 %	6.33 %	5.78 %
4.299E-04	2.04 %	4.769E-04	---	4.231E-04	3.37 %	12.72 %	1.59 %

Table 3. Cross checks of gauge operations.

7. ION GAUGES

Ionization gauges, (ion gauges) are available in several designs. For the system used in this research a glass tube ion gauge similar to Fig. 6 was used for system control, and two metal case ion gauges were used for calibrations at SRSL. The installed glass gauge was typically observed to be in error by a factor of two or more, and accordingly was not evaluated in detail for this study. The accurate metal case ion gauges were Granville Phillips, Model 370, ion gauges (M&TE numbers: SL-457U and SL-457T).

In an ion gauge, a glowing, negatively charged filament is heated using a 280 Volt potential to cause a cloud of electrons to be attracted to a spiraling grid and cylindrical collector. The positively charged grid acts to increase the number of ionizations and magnify the signal output of the gauge. Electrons pass the grid to the positively charged collector to induce an electric current, which is proportional to the pressure in the gauge. The gauge controller then processes the current signal to display a vacuum reading.

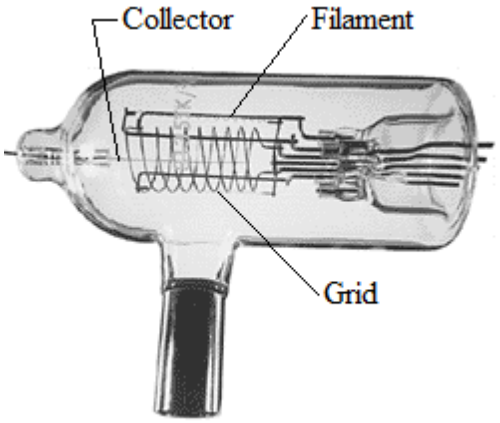

Figure 6. Glass tube ion gauge [14] (Adapted by permission of Scientific Instrument Services).

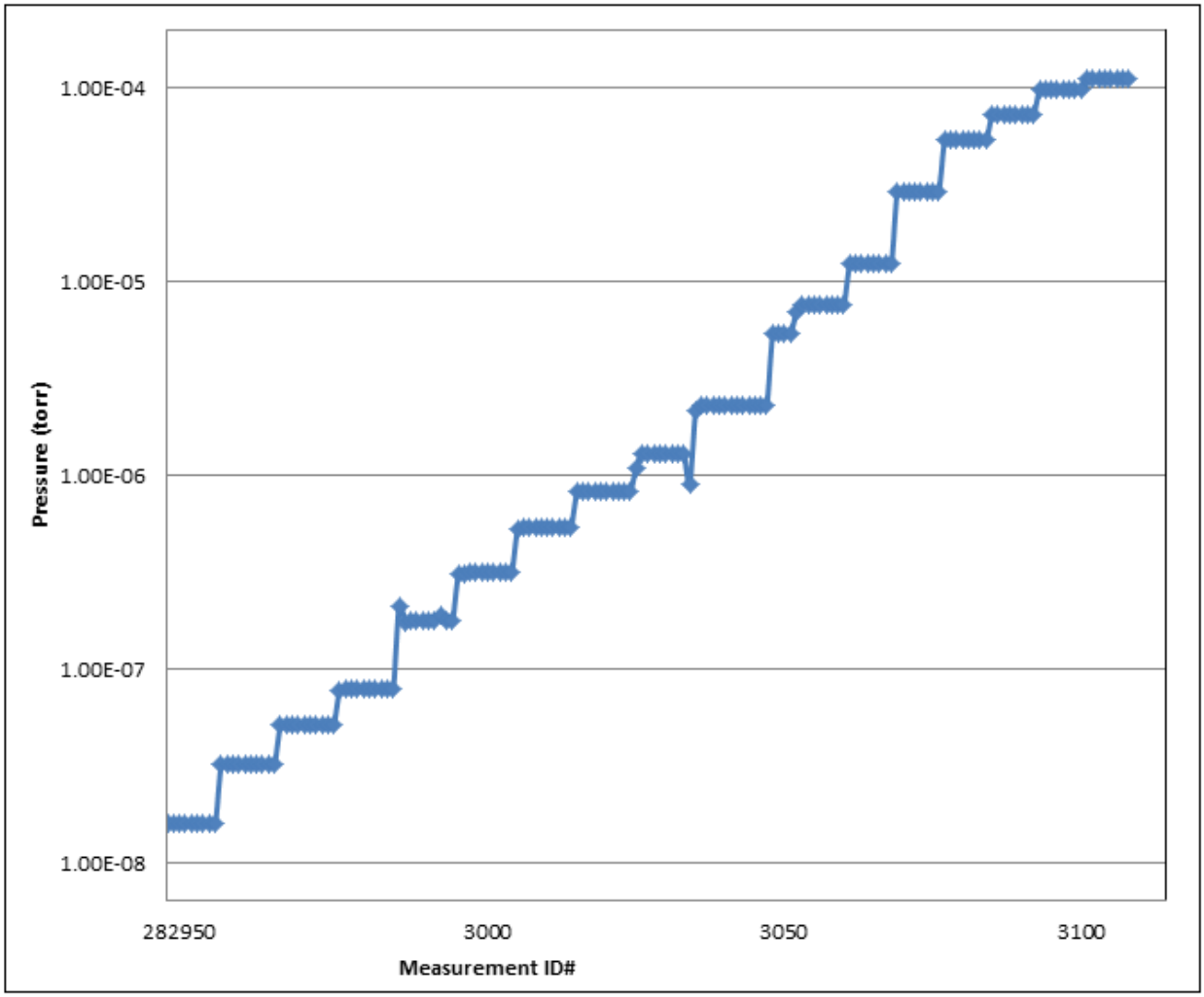

Figure 7. Typical PSL calibration data for an ion gauge (SL-457T) (PSL data provided by Jay Bennett).

7.1 IG Calibrations

IG calibrations are performed at PSL for SRSL, where typical collected data is shown in Fig. 7. PSL provided calibration reports specifying the total uncertainty for each pressure that is measured. Note that pressures are measured while the chamber pressure is increased. Actual pressures were determined at SRSL from these gauges in accordance with Eq. (2).

7.2 IG Test Results

When calibrations are performed after the system was idle for a week or so, the measured pressures were well within uncertainties as shown in Fig. 8. For one gauge, equilibrium was not reached for several days. In other words, calibrations may typically be performed after the system has reached equilibrium for about a week. Also, when this particular system is started up from a shutdown, a one week, or so, delay was usually required to obtain minimum pressures as the system outgassed and moisture contaminants evaporated from internal surfaces. This delay was required to ensure that outgassing did not affect test results. Once the system is outgassed, it remains in continuous operation. For the research performed here, final testing was performed after several weeks of system operation at its lowest operating pressure. Shorter start-up times may affect low pressure measurements.

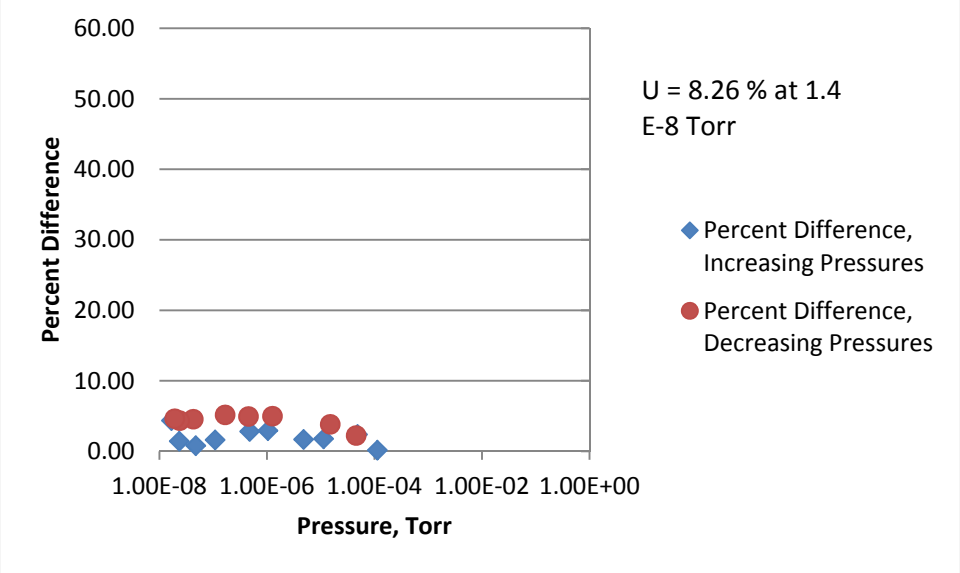

Figure 8. Comparison for IG percent of reading errors following startup, prior to a sudden pressure drop applied to the system (Calibration of SL-457T with a SL-457U standard).

After calibrations were performed, and pressures were suddenly lowered from 1×10^{-4} Torr to ~1×10^{-8} Torr, the percent difference between gauge readings on two separate ion gauges significantly exceeded the total uncertainty, *U*, as shown in Fig. 9. These results were consistent throughout multiple tests, and on occasion the percent difference was 80 % following a pressure drop. Percent differences even increased later the same day during a test that followed the test

shown in Fig. 8. There is no doubt that sudden pressure drops in systems affect pressure readings for ion gauges.

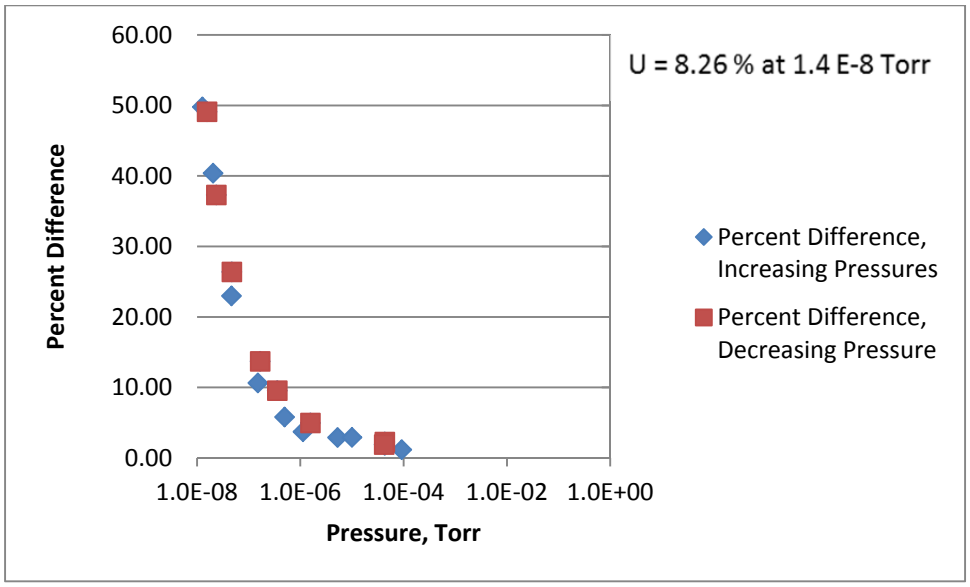

Figure 9. IG pressure differences after a sudden pressure drop was applied to the system (Calibration of SL-457T using SL-457U standard).

However, the magnitude of a pressure drops required to significantly affect pressure readings were not fully investigated, but pressure differences were noted for pressure drops as small as an order of magnitude in pressure. Note also, that percent differences (percent errors for readings) are not significant until pressures drop below 5×10^{-6} Torr. If sudden pressure drops occur in any given system, the gauge user should evaluate the uncertainty effects if gauge accuracy is of significant import.

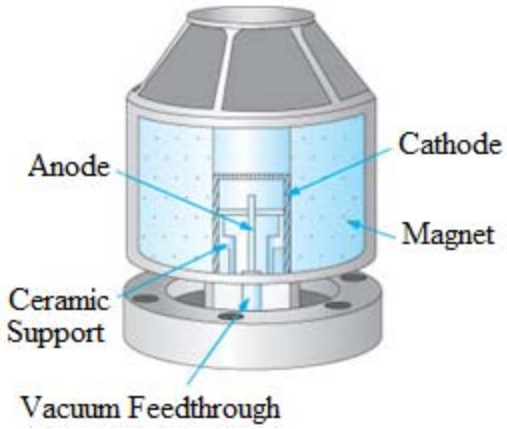

Figure 10. Typical cold cathode design, Lesker [15] (Reprinted by permission of Kurt J. Lesker Company).

8. COLD CATHODE GAUGES

Many years of CCG calibration failures at SRSL prompted this investigation. SRSL performed procedures correctly, and calibration standards were traceable to national standards, but gauges continued to fail calibrations. For years, contamination was considered to be the sole cause of gauge calibration failures. Corrosion and saturation of electrodes have been reported by vendors as possible sources of measurement errors at low pressures following storage at atmospheric conditions, and corrosion been evidenced during calibrations at SRSL. This study discovered an additional cause of incorrect vacuum gauge readings for cold cathode gauges, where sudden drops in pressure resulted in significant gauge errors. This cause of incorrect gauge readings was previously unknown to manufacturers, national laboratories and vacuum system users. In fact, a literature review did not yield any research in this area of molecular flow fluid transients.

Inside the cold cathode gauge, a combination of DC voltage and stationary magnets cause electrons to travel in long spiraling orbits. Moving electrons then ionize other electrons in the CCG to induce measurable voltages, which are converted to pressures by a processor. The basic components of a CCG are shown in Fig. 10. A Pfeiffer, PKR 251 cold cathode gauge was evaluated during this research (M&TE number: 129-PE-K).

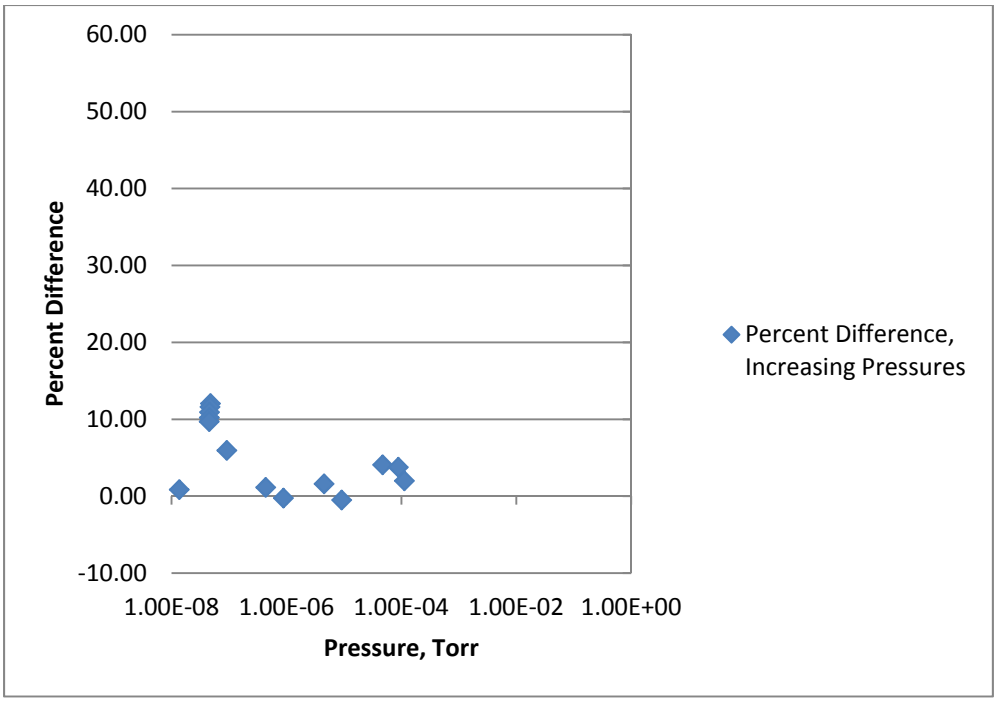

Figure 11. Comparison for measurement errors for a CCG prior to a system pressure drop (129-PE-K, Calibrated using a SL-457U, IG standard).

8.1 CCG Calibrations

When pressures are not suddenly lowered, reasonable errors between standards and CCG's may be obtained. The example shown in Fig. 11 compares an IG to a CCG for an increasing pressure calibration, where an IG was used as the laboratory standard for calibration performance.

8.2 CCG Test Results

Typical test results for a CCG are shown in Figs. 11, 12 and 13, where a new CCG was compared to a laboratory standard IG. Constant uncertainties for CCGs were typically reached in three to five hours, following a sudden pressure drop. However, constant pressures were not obtained until more than a day passed, as shown in Fig. 13. Even so, note that errors are still significant (49.2 %) after a single day of gauge operation following a transient. During low pressure transients, CCG's have the highest uncertainties of the gauges considered. This fact, is attributed to the complex flow path associated with the molecular flow entering the CCG for measurement, where CCG's have the most restrictive flow path of the gauges investigated.

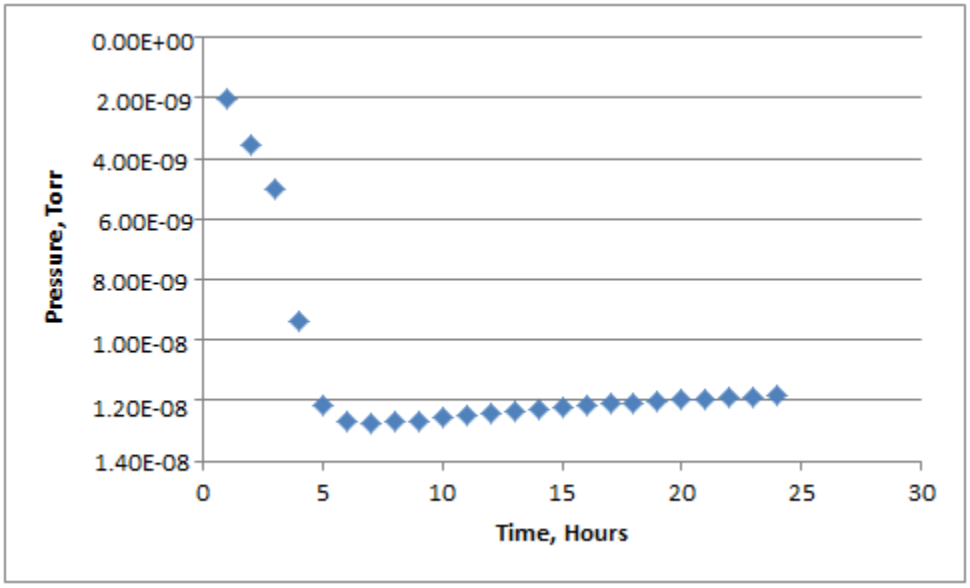

Figure 12. Gauge pressures following a pressure drop in a CCG (129-PE-K, Calibrated using a SL-457U IG, standard).

Corrosion of CCG's is also a significant problem during storage. Figures 11 through 13 provide calibration data for a new, as purchased, gauge. Figure 14 provides calibration data for that same gauge which was calibrated a second time after a year of storage. This one year calibration was performed following a four day installation prior to calibration to ensure that equilibrium was obtained for the CCG in the vacuum system. Compare Fig. 11 to Fig. 14 to note that percent differences for gauge readings increased by as much as an order of magnitude from 12.0 % to 121.7 %. This significant increase in gauge error was attributed to corrosion due to a year of storage on the shelf, where the gauge was subject to changing humidity. Corrosion

effects were also noted during previous calibrations at SRSL for gauges that were subject to extended storage, where cleaning of gauges tended to lower gauge errors. Corrosion effects were not investigated while gauges were installed at vacuum, but as-installed corrosion effects on cold cathode gauges should be negligible due to extremely low moisture content in vacuum systems.

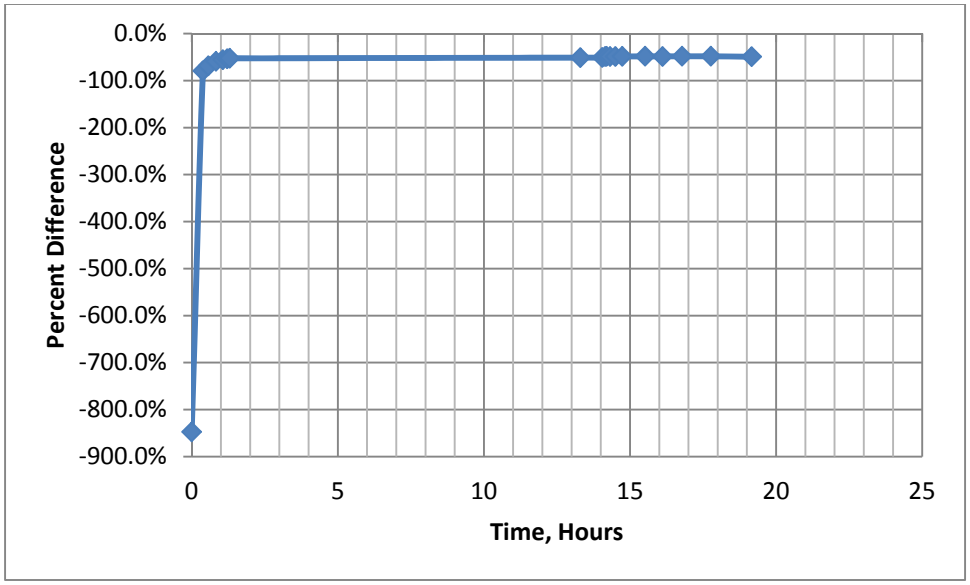

Figure 13. CCG performance following a pressure drop (129-PE-K, Calibrated using a SL-457U, IG standard).

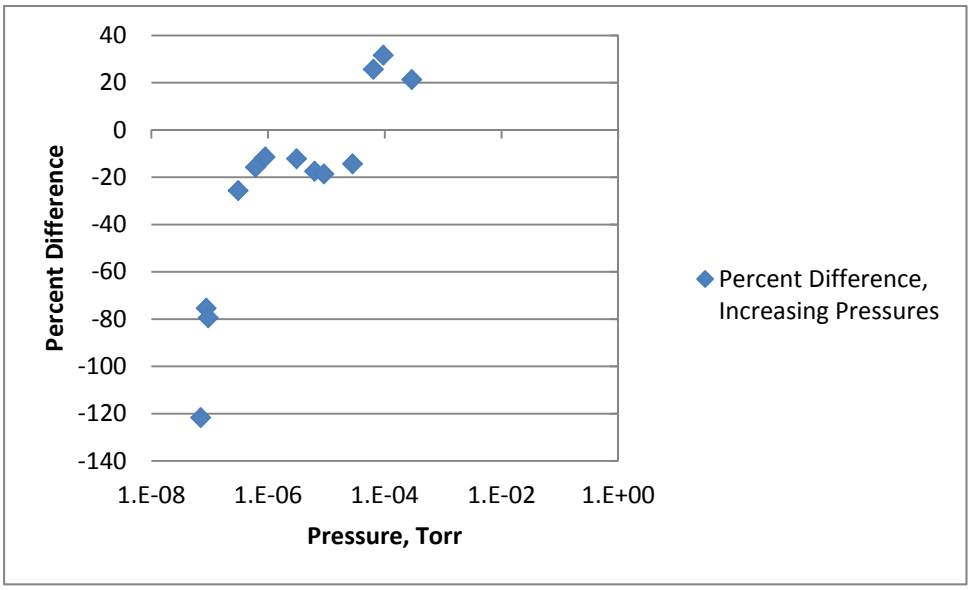

Figure 14: CCG Measurement Errors Following One Year of Shelf Storage (129-PE-K, Calibrated using a SL-457U, IG standard).

9. SPINNING ROTOR GAUGES

In spinning rotor gauges, drag is caused by gas molecules passing over a magnetically levitated, spinning steel sphere. A residual drag across the rotating sphere is measured, and this drag is used to establish the pressure in the system. An MKS Instruments, SRG-3CE, spinning rotor gauge was used for this research (M&TE number: SL-456G).

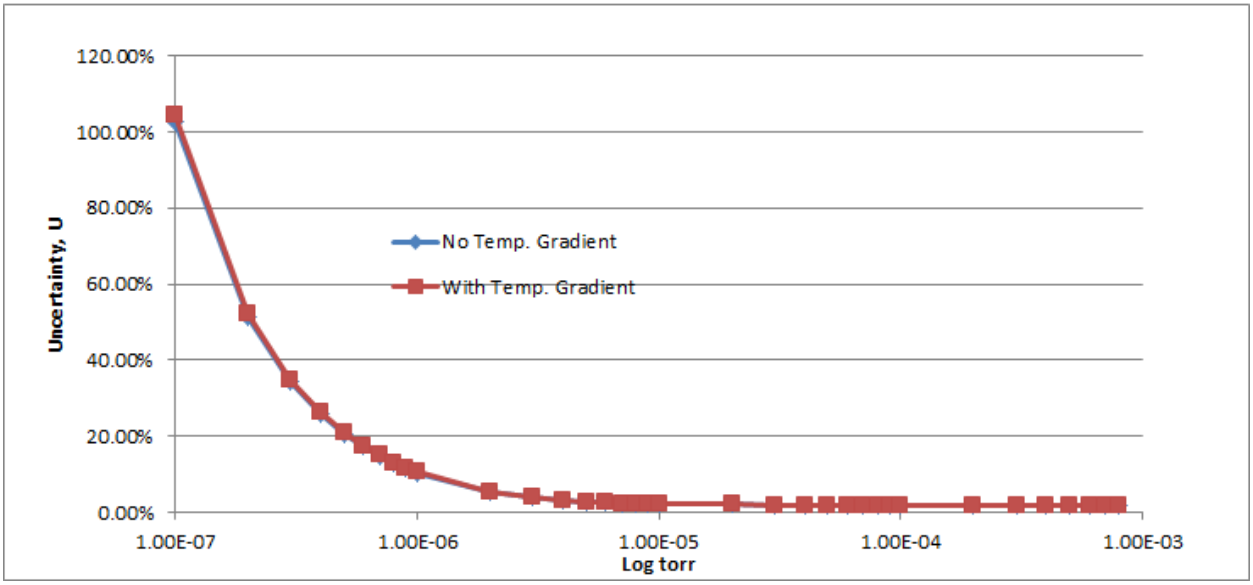

Figure 15. SRG uncertainties (Calibration of SL-456G with a SL-457U, IG standard).

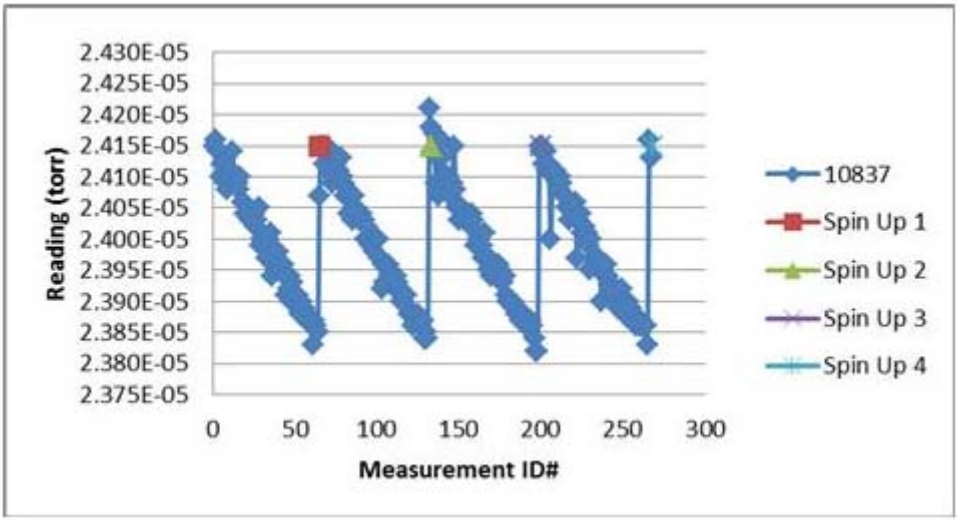

Figure 16. Ball rotation effects on an SRG (PSL data provided by Jay Bennett).

9.1 SRG Calibrations

SRG's are calibrated by NIST for SRSL where multiple measurements are performed at a single pressure, using a primary transition-range vacuum standard which generates a known pressure by

transmitting a known flow rate through an orifice of known area. The PSL uncertainty at this pressure is augmented by Excel® spread sheets to calculate uncertainties throughout the range of use. Uncertainties for the ball diameter, gas and temperature were included, as provided by James Fedchak of NIST. The effects of these uncertainties are shown in Fig. 15, where $U = 3.64$ Torr for this test. Additionally, PSL has noted that there are additional uncertainties due to ball rotational effects as depicted in Fig. 16, which were not separately considered in the NIST uncertainty analysis that was used to obtain Fig. 15. However, this ≈1 % uncertainty observed in Fig. 16 was effectively included in the overall uncertainty calculation for the SRSL calibration process. All in all, SRG uncertainties are quite excessive. When an ion gauge was compared to an SRG, the errors were much higher than expected, where vendor literature that stated that $U =$ 2.6 % between 1.3×10^{-7} and 1.3×10^{-4} Torr, during a one year period. SRG experimental uncertainties agree reasonably well with the NIST uncertainties depicted in Fig. 15. In other words, SRG's may have high uncertainties when operating pressures are below about 5×10^{-6} Torr.

9.2 SRG Test Results

Initial SRG tests were performed after the system was operated without pressure drops for two days. Numerous tests with SRG's provided similar results. For these tests, the pressures are incrementally increased from approximately 1×10^{-8} Torr to 10×10^{-4} Torr, and then incrementally decreased back down to 1×10^{-8} Torr, where the percent errors (percent differences) are shown for these increasing and decreasing pressure calibrations. Typical error results are shown in Fig. 17.

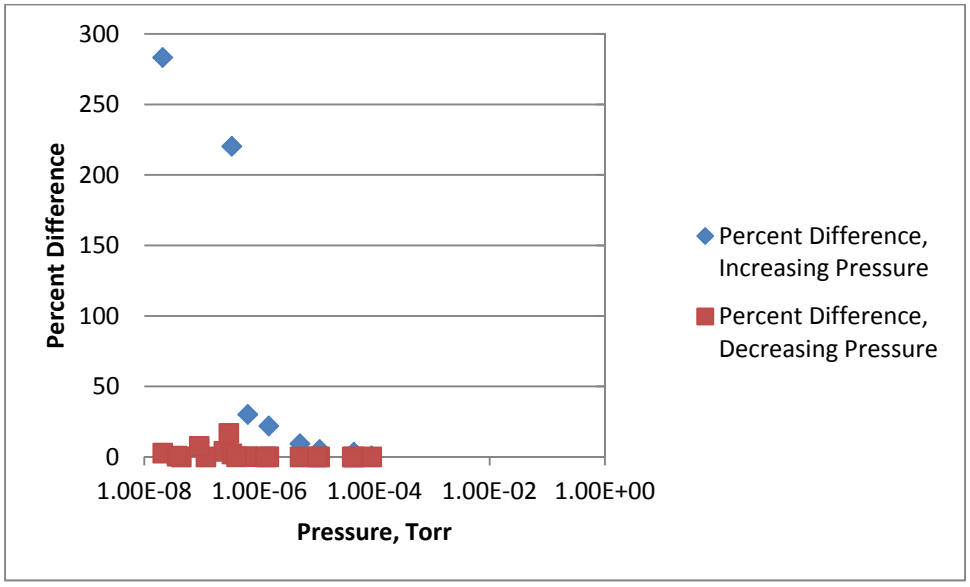

Figure 17. SRG performance for an increasing pressure calibration and before a sudden pressure drop was applied to the system (Comparison of SL-457U to SL-456G standards).

Figures 8 and 17 may be used to compare gauge performance for IG's and SRG's with respect to error performance. Typical pressure vs. measurement errors are shown in Fig. 17, where an SRG was calibrated with an IG standard. By comparison, test results from Fig. 8 showed that ion gauges performed much better at these pressures with respect to errors. Figure 8 and Fig. 17 data were collected together, while two IG's and the SRG were connected to the chamber and operating. In other words, testing at the same time, under the same conditions, showed that SRG uncertainties were much higher than IG uncertainties at high vacuum.

Then when the pressure was then suddenly lowered in the vacuum system several hours later, pressures were measured again. Measurement errors increased at low pressures as shown in Fig. 18. For this test, the pressures were also incrementally raised and lowered during the calibration, which used an ion gauge standard to perform the calibration. By comparing Figs. 17 and 18, note that the errors increased, which concluded that sudden pressure changes significantly affected SRG performance at low vacuum. Higher uncertainties during pressure transients for the SRG are attributed to the fact that the entrance tubing from the vacuum chamber to the SRG is longer and of smaller diameter than the entrance tubing to the ion gauge. That is, the molecular flow has a more difficult and restrictive path to enter the SRG than it does to enter the IG.

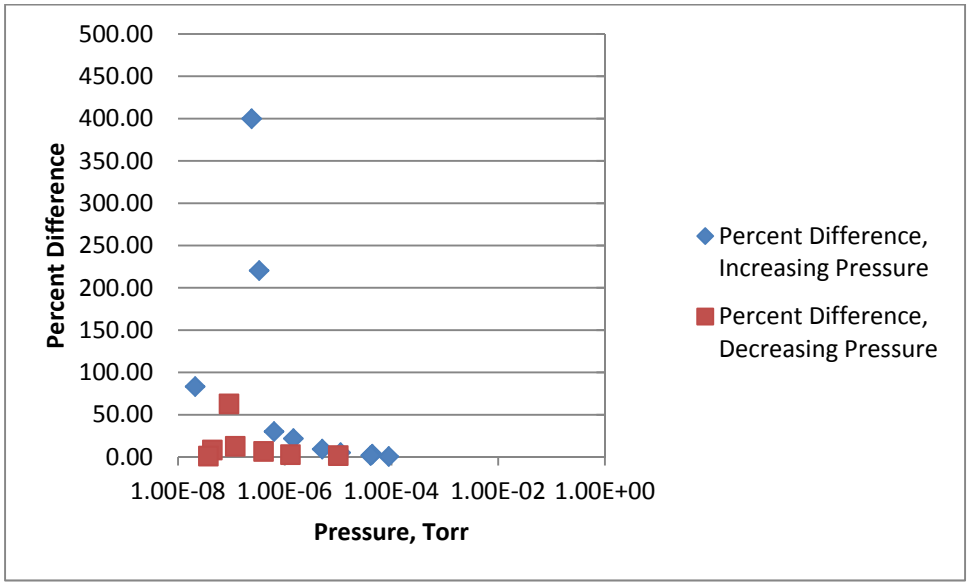

Figure 18. SRG performance for an increasing pressure calibration, after a sudden pressure drop was applied to the system (Comparison of SL-457U to SL-456G standards).

10. FLUID TRANSIENTS

Fluid transients are reasonably well understood for cases where the fluid is a liquid or gas, which acts as a continuum (Leishear [16]). However, transient pressures and transient flow rates in molecular flow cannot be described using continuum mechanics, and therefore molecular flow, fluid transients are little understood.

Even so, velocities in the tubing can be approximated by Eq. (8) to provide some insight into what happens when pressures are suddenly changed in vacuum systems and gauges. Different gauges can be represented by using tubing diameters and approximate tubing lengths. The initial velocity, V, can be determined by combining the cross sectional area, A, in cm^2 of the tubing with the conductance from Eq. (8) to obtain

$$V = \frac{C}{A \cdot 100} = \left\{ \frac{135 \cdot d^4 \cdot \left(\frac{p_1+p_2}{2}\right)}{L} + \frac{12.1 \cdot d^3}{L} \cdot \frac{1+192 \cdot d \cdot \left(\frac{p_1+p_2}{2}\right)}{1+237 \cdot d \cdot \left(\frac{p_1+p_2}{2}\right)} / A \right\} m/s. \quad (9)$$

Using Eq. (9), the approximate velocity can be determined as gas enters or exits the chamber from different gauges at the time when pressures are suddenly lowered, where p_1 and p_2 are assumed to be the pressures in a gauge or in the chamber as applicable. Approximate lengths and diameters were measured from the installed equipment. Table 4 provides calculated initial velocities of gas entering or exiting the chamber to or from different gauges for a single, common set of selected pressures, p_1 and p_2.

From the data in Fig.4, note that velocities for different gauge designs are 1000 to 1 million times faster when chamber pressures are decreased in the 1×10^{-4} Torr range and 1×10^{-8} Torr, respectively. In other words, flow rates are orders of magnitudes smaller at high vacuum. This difference in flow rate is coincident to experimental results to definitively prove that sudden pressure drops cause significant vacuum gauge errors at low pressures. Effectively, the probability of molecules exiting a gauge is higher than the probability of molecules reentering a gauge. Within the gauge and attached tubing, molecules reflect off of the surfaces to collimate the stream of molecules exiting the gauge, and increase the average drift velocity of the molecules. Once the molecules exit the gauge into the chamber, this collimation effect that increases the average velocity in a confined space is not present. Gas molecules randomly enter the chamber wall opening into the gauge tubing, and the average velocity is therefore lower when the gauge is filling than when it is venting. Apparently these random molecular effects on flow rates are only significant for low pressures coupled with sudden pressure decreases.

Considering the CCG, it has a slower response time to return to equilibrium than ion gauges. The narrow passages and orifice plates found in CCG's provide an explanation for this slower response. Molecular flow is simply more restricted in a CCG than an IG, and the flow rate from the gauge is reduced even further.

Consider the chamber and gauges to examine these conclusions with respect to pressure drops. When the system is fully evacuated to $\sim 1 \times 10^{-8}$ Torr and then pressurized slightly, the evacuated gauge and chamber fill together, while the gauges fill at slower rates. The tank is at a higher pressure than the gauges and provides a nearly constant velocity flow into the gauges, since the tank volumes are negligibly affected as indicated by the ratio of gauge volume to chamber volume in Table 4. Each additional calibration is performed in turn until the pressure

reaches 1×10^{-4} Torr. Then the chamber is vented back to ~1×10^{-8} Torr. Now, the chamber has no resistive force to flow from the velocity flow from the gauges, and the gauges vent their pressure nearly asymptotically. Unless sufficient time is permitted to fully vent the gauges, residual pressures are present in the gauges when the system is re-pressurized. Then as the system increases pressure, opposing molecular flows occur within the gauges; one flow from the chamber, one opposing flow from the gauge components. Once gas molecules are removed from a gauge at low pressures due to pressure surge from the vacuum system, molecules are slow to refill the gauges. The lower gas density in the gauge then affects gauge readings until equilibrium between the tank and the gauge is reestablished. Accordingly, transient molecular flows affect the uncertainty and error of the gauges, where experimental testing demonstrated this conclusion.

Gauge	Velocity, m/sec	Conductance, liters/second	p_1, Tank Pressure, Torr	p_2, Gauge Pressure, Torr	d, cm	L, cm	Ratio of (Gauge + Tubing Volume) / (Chamber Volume)
IG	1.270E-06	1.217E-03	5.95E-08	2.49E-08	3.493	12.700	0.0243331
SRG	5.613E-08	7.110E-06	5.95E-08	2.49E-08	1.270	38.100	0.0096528
CDG	1.901E-09	1.505E-08	5.95E-08	2.49E-08	0.318	71.120	0.0011261
CCG	4.886E-07	4.681E-04	5.95E-08	2.49E-08	3.493	33.020	0.0632660
IG	6.725E-03	6.442E+00	5.73E-04	1.10E-04	3.493	12.700	0.0243331
SRG	3.336E-04	4.226E-02	5.73E-04	1.10E-04	1.270	38.100	0.0096528
CDG	1.193E-05	9.449E-05	5.73E-04	1.10E-04	0.318	71.120	0.0011261
CCG	2.586E-03	2.478E+00	5.73E-04	1.10E-04	3.493	33.020	0.0632660

Table 4. Initial gas velocities between the gauges and chamber.

11. RECOMMENDED CORRECTIVE ACTIONS

To improve gauge performance at low pressures, several precautions should be observed:

1. Ensure that the system is at equilibrium before starting a calibration, which may take a day to a week, or so, between calibrations at high vacuums. This delay is in addition to the start-up delay before calibrations that is usually required to outgas the vacuum system after extended outages after the system is subjected to atmospheric humidity.
2. Perform calibrations for increasing pressures only.
3. Reduce pressures slowly to prevent vacuum gauge errors.
4. Evaluate specific vacuum systems for fluid transients due to suddenly lowered pressures. The effects of system volume on transient pressures were not evaluated during this research.
5. Do not measure vacuum pressures immediately following sudden pressure decreases in a system.

12. CONCLUSIONS

Conclusive testing proved that sudden pressure drops in vacuum systems significantly affect vacuum gauge readings for different vacuum gauge designs, which included ion gauges, spinning rotor gauges and cold cathode gauges. The cause of this anomaly is attributed to rapid changes in molecular flow and the inability of the vacuum system to immediately return to equilibrium at low pressures approaching 1×10^{-8} Torr. These effects on gauges are geometry dependent, where cold cathode gauges that are more affected by restricted flow paths inside the gauge as compared to spinning rotor gauges that have less restricted flow paths or ion gauges that have even less restricted flow paths which are fully open to the vacuum chamber. In short, uncertainties far exceed manufacturers published uncertainties when pressures are suddenly lowered to high vacuum for several different gauge designs during low pressure molecular flow fluid transients. Additionally, SRG uncertainties were found to increase significantly below 5×10^{-6} Torr. Although additional research is warranted, sufficient data has been collected to support these conclusions.

To minimize measurement accuracy errors during routine vacuum gauge calibrations, ensure that the system has reached its lower operating limits before performing measurements, validate gauge accuracy before proceeding with calibrations, and then only perform measurements while increasing the system pressures. These actions control fluid transient effects on gauge accuracy when pressures are suddenly decreased.

To minimize measurement accuracy errors during vacuum system operations, vacuum system users may need to evaluate the time required for their system to return to equilibrium following a fluid transient caused by suddenly decreasing pressures.

13. ACKNOWLEDGEMENTS

Jay Bennett and Mark Benner of the Primary Standards Laboratory at Sandia National Laboratories in Albuquerque, New Mexico and James Fedchak of NIST in Gaithersburg, Maryland are gratefully acknowledged for their contributions with respect to SRG calibrations. Research was performed in the Savannah River Standards Laboratory, which is operated by the Savannah River National Laboratory for the U.S. Department of Energy in Aiken, South Carolina.

14. REFERENCES

[1] *ISO/IEC 17025*, "General Requirements for the Competence of Testing and Calibration Laboratories," International Organization for Standardization, Geneva, Switzerland, 2005.

[2] *JCGM 100*, "Evaluation of Measurement Data – Guide to the Expression of Uncertainty in Measurement", Bureau International des Poids et Mesures, Sevre Cedex, France, 2008.

[3] B. Taylor and C. Kuyatt, "NIST Technical Note 1297, Guidelines for Evaluating and Expressing the Uncertainty of NIST Measurement Results, National Institute of Standards and Technology, Gaithersburg, Maryland, 1994.

[4] *ASME B89.7.3.1*, "Guidelines for Decision Rules: Considering Measurement Uncertainty in Determining Conformance to Specifications", American Society of Mechanical Engineers, New York, New York, 1989.

[5] H. Colemen and W. Steele Jr., *Experimentation and Uncertainty Analysis for Engineers*, John Wiley and Sons, New York, New York, 1989.

[6] *ISO/TS 3567-2005*, "Vacuum gauges, Calibration by direct comparison with a reference gauge", International Organization for Standardization, Geneva, Switzerland.

[7] *ISO 27893-2011*, "Vacuum technology — Vacuum gauges — Evaluation of the uncertainties of results of calibrations by direct comparison with a reference gauge", International Organization for Standardization, Geneva, Switzerland.

[8] Varian, Inc., *Basic Vacuum Practice*, Lexington, Massachusetts, 1989.

[9] Boltzman, L., *Lectures on Gas Theory*, University of California Press, Berkeley, California, 1964.

[10] W. Umrath, *Fundamentals of Vacuum Technology*, Oerlikon, Cologne, Germany, 2007.

[11] Pfeiffer Vacuum, "The Vacuum Technology Book, "Part 2: Know-how book", http://www.pfeiffer-vacuum.com (last accessed December 2014).

[12] J. John, 1984, *Gas Dynamics*, Allyn and Bacon, Newton, Massachusetts.

[13] Omega Engineering, Inc. Stamford, Connecticut, http://www.omega.com/literature /transactions/volume3/high3 .html (last accessed, March, 2015).

[14] Scientific Instrument Services, Ringoes, New Jersey, http://www.sisweb.com/vacuum/sis /inlinga.htm (last accessed March 2015)

[15] Kurt J. Lesker Company, "Pressure Measurement Technical Notes," Pittsburg, Pennsylvania, http://www.lesker.com/newweb/gauges/gauges_technicalnotes_1.cfm, (last accessed December 2014).

[16] R. Leishear, *Fluid Mechanics, Water Hammer, Dynamic Stresses, and Piping Design,* American Society of Mechanical Engineers, New York, New York, 2013.